Science Advances

AAAS

advances.sciencemag.org/cgi/content/full/3/2/1602067/DC1

Supplementary Materials for

Fragmentation of wall rock garnets during deep crustal earthquakes

Håkon Austrheim, Kristina G. Dunkel, Oliver Plümper, Benoit Ildefonse, Yang Liu, Bjørn Jamtveit

Published 22 February 2017, *Sci. Adv.* **3**, e1602067 (2017)
DOI: 10.1126/sciadv.1602067

This PDF file includes:

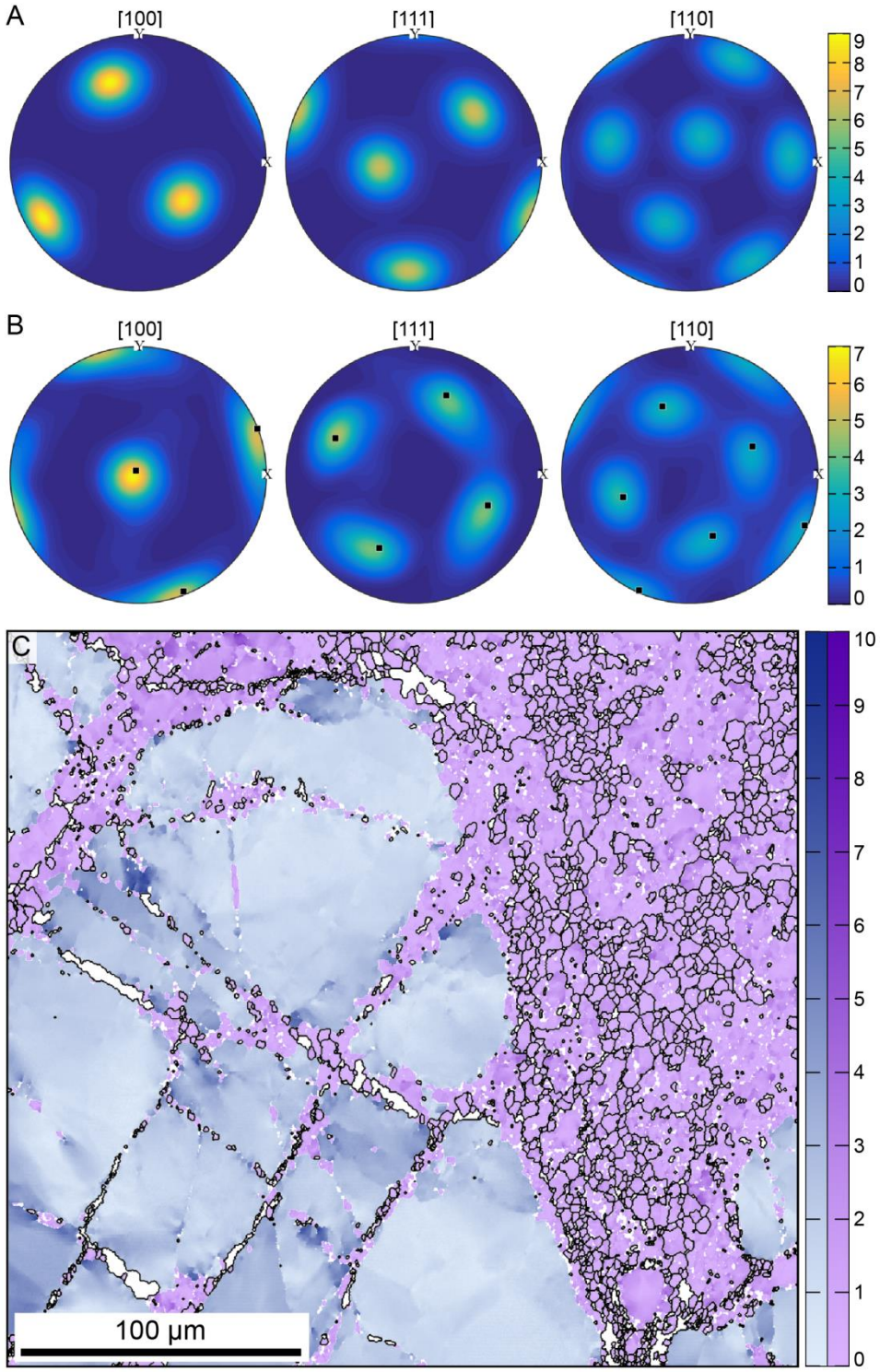

fig. S1. Strong CPOs of fragmented garnets. (**A**) Equal-area lower-hemisphere stereographic projections of the orientation distribution function (ODF) of garnet in the domain of Grt I. (**B**) ODF of strongly deformed garnet with subgrain sizes ≤ 600 µm^2 in the domain of Grt II. Black squares denote the orientations of maxima in the ODF of the comparatively undeformed garnet of the same area with subgrain sizes > 600 µm^2. (**C**) Misorientation map of Grt II. The misorientation angle of each pixel is given in degrees relative to the mean orientation of the subgrain it belongs to. Garnet with subgrain sizes > 600 µm^2 is in blue; garnet with subgrain sizes ≤ 600 µm^2 is in pink. Garnet grain boundaries are superimposed in black. White areas are secondary phases.

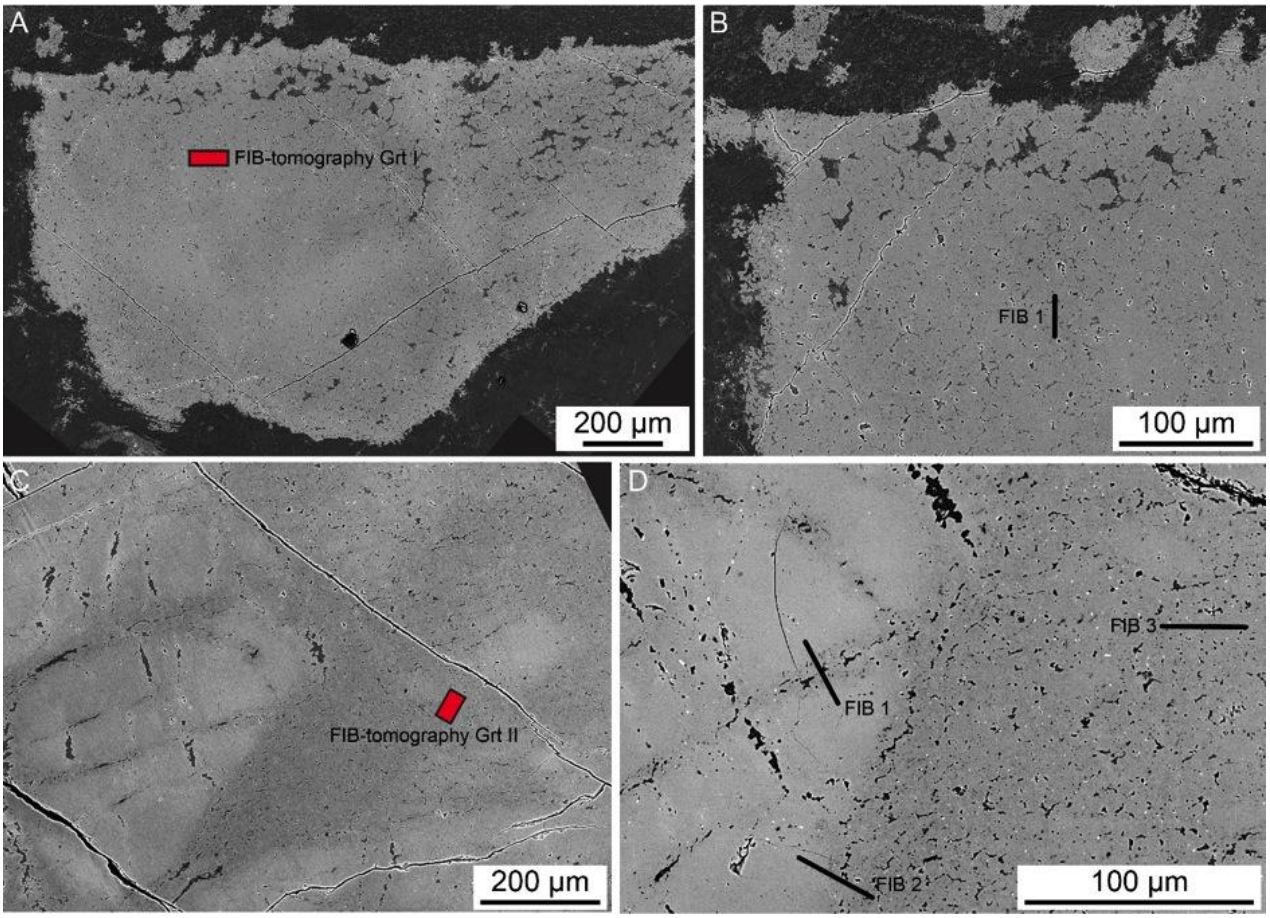

fig. S2. Position of nanotomography volumes and TEM lamellae. Backscattered electron (BSE) images collected with a focused ion beam scanning electron microscope (FIB-SEM) showing the location of the FIB-SEM tomography and the TEM lamellae excavation of (**A**)-(**B**) Grt I and (**C**)-(**D**) Grt II.

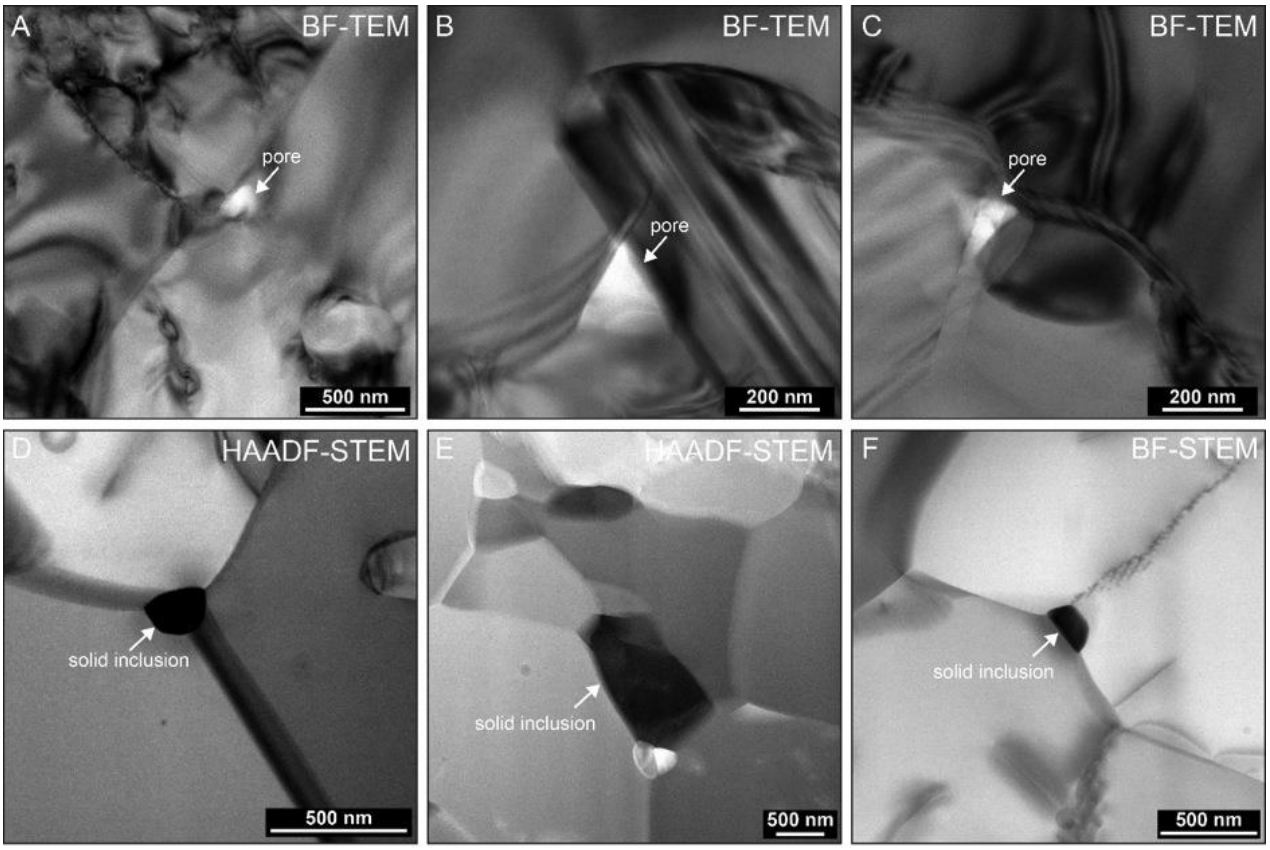

fig. S3. TEM images of pores and inclusions. (**A**)-(**C**) Bright-field (BF-) transmission electron microscopy (TEM) images of isolated pores at grain boundaries within the fragmented garnet domains in the vicinity of the pseudotachylite-bearing fault. (**D**)-(**F**) High-angle annular dark field (HAADF) and BF scanning TEM (STEM) images of solid inclusions at grain boundary triple junctions within the fragmented garnet domains.

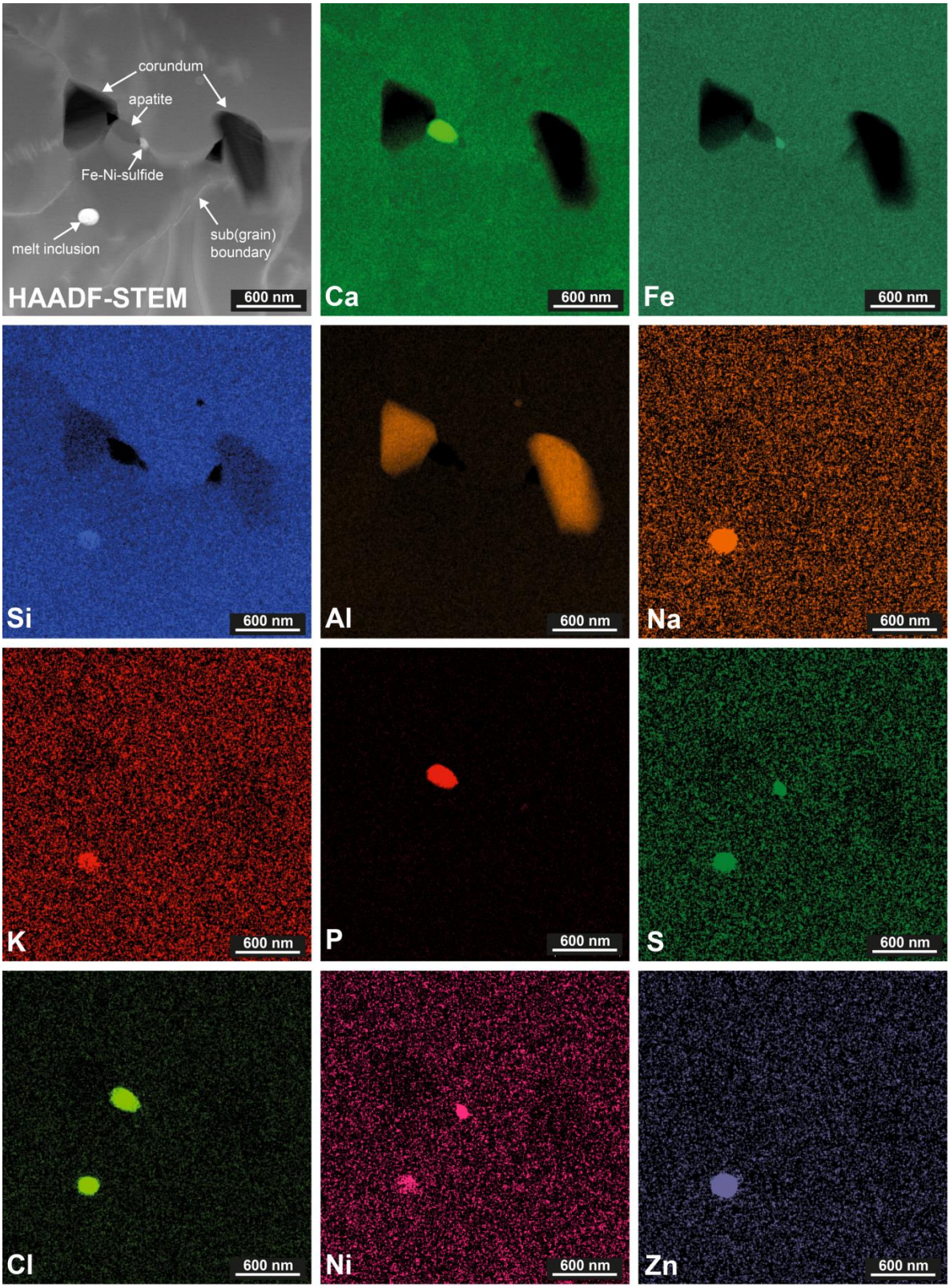

fig. S4. Inclusion phases in fragmented garnet. Chemical mapping of inclusions along (sub)grain boundaries in Grt I. The top left image is a high-angle annular dark-field (HAADF) image recorded in scanning transmission electron microscopy (STEM) mode giving an overview about the mapping area. The following images are energy-dispersive X-ray (EDX) maps taken with a Talos 200FX equipped with a SuperX EDX system. The pixel size is 3 nm. From this chemical map 4 different types of inclusions can be identified, corundum, apatite, Fe-Ni-sulfide and a melt inclusion. A detailed analysis of the melt inclusion can be found in fig. S7.

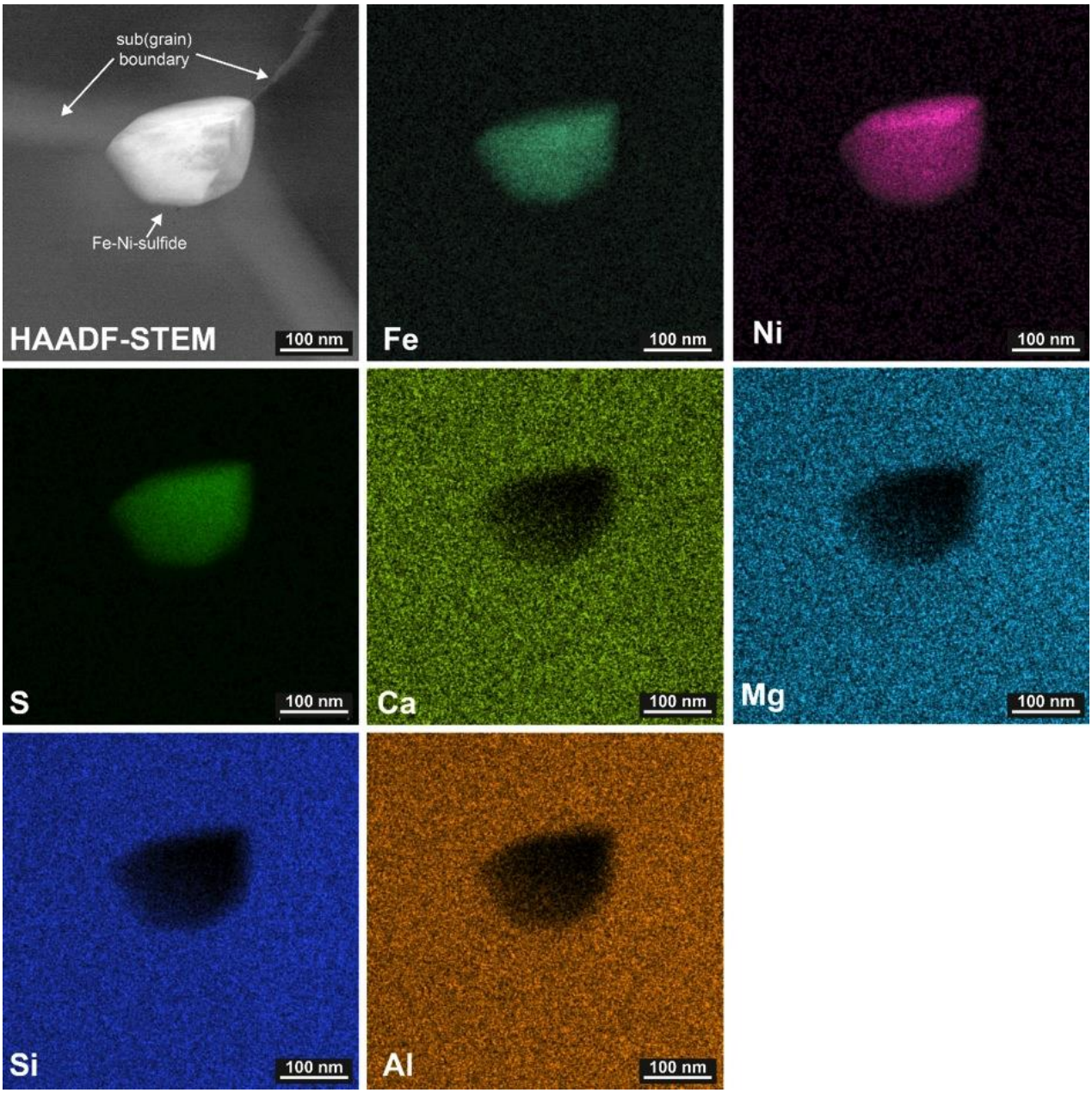

fig. S5. Sulfide inclusion in garnet. Top left image is a high-angle annular dark-field (HAADF) image recorded in scanning transmission electron microscopy (STEM) mode showing a Fe-Ni-sulfide at a sub(grain) boundary triple junction. The following images are energy-dispersive X-ray (EDX) maps recorded in scanning transmission electron microscopy (STEM) mode.

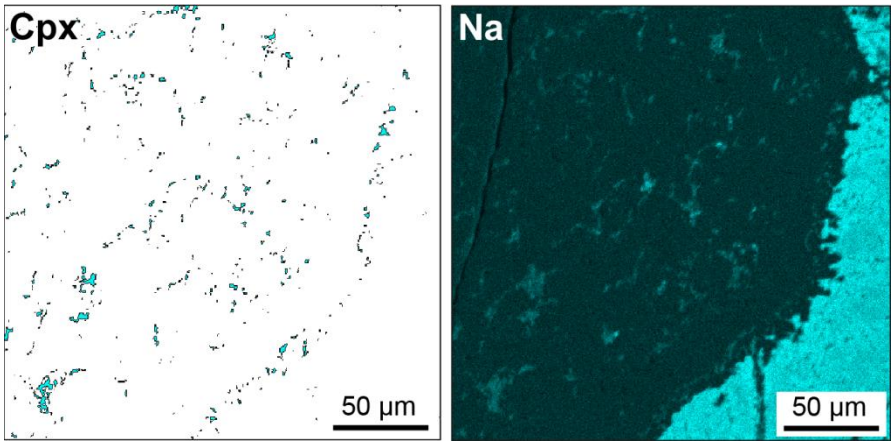

fig. S6. Clinopyroxene inclusion distribution and composition. The left panel shows the positions of clinopyroxene as determined by EBSD analysis. Most of it was indexed as diopside, but the distinction between diopside and omphacite is unreliable because of their very similar crystal structures. The qualitative Na map in the right panel shows that the clinopyroxene contains Na, indicating that it is omphacite or sodic augite.

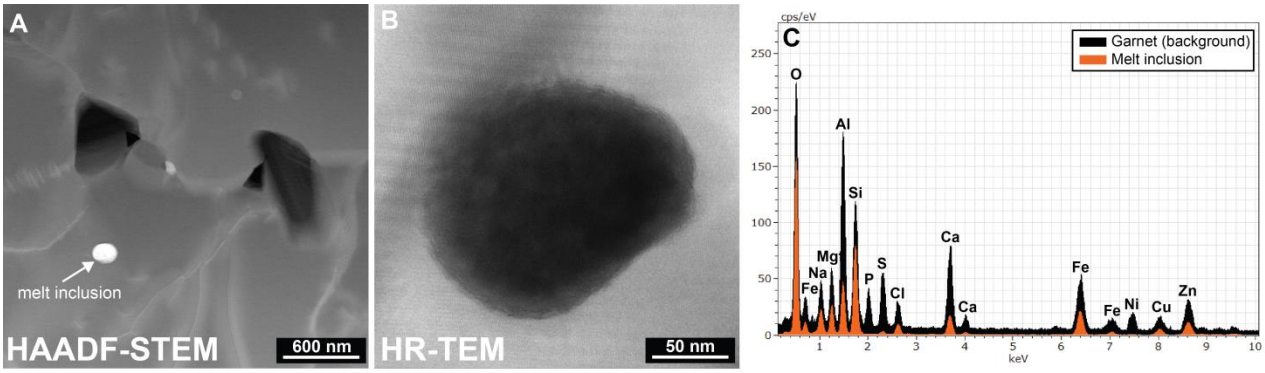

fig. S7. Melt inclusion along (sub)grain boundary in fragmented garnet. (**A**) High-angle annular dark-field (HAADF) image recorded in scanning transmission electron microscopy (STEM) mode showing the location of a representative melt inclusion. (**B**) High-resolution (HR-) transmission electron microscopy (TEM) images highlighting the amorphous nature of the melt inclusion. Lattice fringes corresponding to the garnet are visible around the melt inclusion, whereas the inclusion shows no lattice fringes, confirming its amorphous nature. (**C**) Energy-dispersive X-ray (EDX) spectrum of the melt inclusion compared to the garnet surrounding the inclusion. The black EDX spectrum denotes the background spectrum of the entire area shown in (A), whereas the orange EDX spectrum is the melt inclusion. The chemistry of the inclusion is also shown in the EDX map in fig. S4.

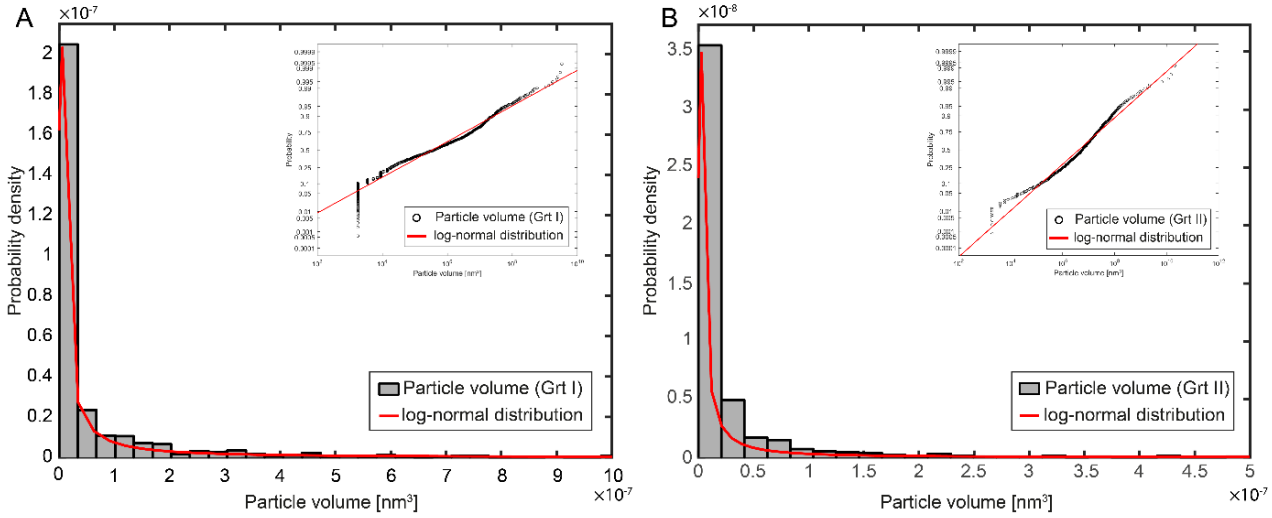

fig. S8. Size distribution of inclusions. Probability histogram of particle volume extracted from focused ion beam - scanning electron microscopy (FIB-SEM) nanotomography from (**A**) Grt I and (**B**) Grt II. The red lines in (A) and (B) are log-normal probability density functions of the particle volumes. Insets are probability plots of the particle volume with corresponding fitted log-normal distribution. The analysis shows that the particle volumes closely follow a log-normal distribution consistent with a nucleation and growth control on their formation.